TRANSIENT PHENOMENA AND OUTBURSTS FROM GALACTIC BLACK-HOLE CANDIDATES

T. Belloni [a]

[a]Osservatorio Astronomico di Brera, Via E. Bianchi 46, I-23807 Merate (LC), Italy

The RossiXTE mission provided us with an unprecedentedly large database of X-ray observations of transient black-hole candidates. These systems are crucial for the understanding of the physical properties of mass accretion onto black holes. Here I review the results on a selected sample of systems and describe their behavior in a purely phenomenological way. From these results, we can derive a better classification of the spectral and timing characteristics of black hole candidates in terms of basic states.

1. Before RXTE: spectral/timing states

Transient black hole candidates (TBHC) are the most important laboratories where we can study accretion onto black holes. The main reasons are two: first, there is a very limited number of bright persistent systems; second, transients go through a large range of mass accretion rate during their outbursts, therefore allowing us to study how the accretion properties change with accretion rate. In the case of persistent sources, they show rare state transitions (if any), and even when they do it is not clear what their dependence on accretion rate is (see e.g. [1]).

Before the launch of the Rossi X-ray Timing Explorer (RXTE), a relatively small number of systems was known (see [2, 3] for a review). From these sources, a general "canonical" paradigm for the spectral/timing properties of TBHC had emerged (see [2, 3, 4]). Although there were notable exceptions, this paradigm was a good starting point for theoretical modeling. Four separate states were identified, which will be described here according to the behavior in the 2-20 keV band:

- Low/Hard State (LS): the energy spectrum can be described by a single power law with a photon index $\Gamma \sim 1.6$. In addition, sometimes a weak disk-blackbody (DBB) component with kT<1 keV is observed, contributing less than a few percent to the detected flux. The Power Density Spectrum (PDS) is characterized by a strong band-limited noise with a break frequency below 1 Hz and a large fractional variability (30-50%). A low-frequency <1 Hz QPO is sometimes observed.

- Intermediate State (IS): the energy spectrum can be decomposed in two components: a power law with $\Gamma \sim 2.5$ and a clearly detectable DBB with kT$\leq$1 keV. The PDS shows a band-limited noise with a break frequency higher than the LS (1-10 Hz) and a fractional variability of 5-20%. Sometimes a 1-10 Hz QPO is observed.

- High/Soft State (HS): the energy spectrum is dominated by a DBB component with kT$\sim$1 KeV, with the power-law component either below detection or extremely weak and steep ($\Gamma \sim 2$–3). Very weak noise is detected in the PDS, in the form of a power-law with a few % of fractional variability.

- Very High State (VHS): the energy spectrum is a combination of a DBB (kT$\sim$1-2 keV) and a power law ($\Gamma \sim 2.5$). The PDS can be of two types: either a band-limited noise similar to that of the IS, or a power-law, sometimes with a QPO. This state was observed only in two sources: the transient GS 1124-68 and the persistent source GX 339-4.

The dependence of these states and their transitions on increasing accretion rate was determined mostly by the only transient system that had shown all four of them, GS 1124-68 [5, 6]: LS–IS–HS–VHS. As one can see from the description above, the IS is very similar to the VHS, both in energy and timing characteristics. What was believed to be different between them is the value of the accretion rate: the VHS was observed at very high accretion rates, while the IS was observed much later in the outburst of GS 1124-68,

after a long period of HS, and therefore at lower accretion rate (see [7]).

Despite the exceptions, a transient was expected to have a fast-rise/exponential-decay light curve (reflecting the time history of accretion rate), lasting a few months, possibly with one or more re-flares, undergo a number of state transitions in the sequence outlined above following accretion rate changes, and return to quiescence after a period of a few weeks to months, until the next outburst. Once again, the prototypical source would be GS 1124-68.

2. The RXTE "outburst"

With the advent of RXTE at the end of 1995 [10, 11], our view of TBHC has been changed and widened. Thanks to the All-Sky Monitor (ASM) on board RXTE [12], we have been able to discover promptly both new transients and new outbursts of known ones. The flexibility of the mission allowed the accumulation of a vaste and valuable database of pointed observations with the narrow field instruments on board, covering the wide range 2-200 keV. In particular, the large collecting area of the PCA instrument [13, 14] yielded high signal-to-noise data for timing and spectral analysis, and the availability of the RXTE archive on-line made these datasets easily accessible to the community. This resulted in a real "outburst" both of new sources and of publications on the subject.

In the rest of the paper, I will concentrate on the results on a few major systems and show how these have changed our overall picture. My approach will be mostly on the phenomenological side.

3. XTE J1550-564

This transient was discovered in September 1998 with RXTE and its outburst lasted until May 1999 (see [8] and references therein). Two more outbursts were detected in 2000 and 2001, but I will concentrate on the 1998/1999 one. As one can see from Fig. 1, the light curves in the PCA and HEXTE instruments look quite different, indicating large spectral changes.

A complete spectral analysis of these data can be found in [8]. However, the second part of this outburst (after MJD 51139, see Fig. 1) was analyzed in terms of color-color diagrams (CCD) by [9], showing in a model-independent way the

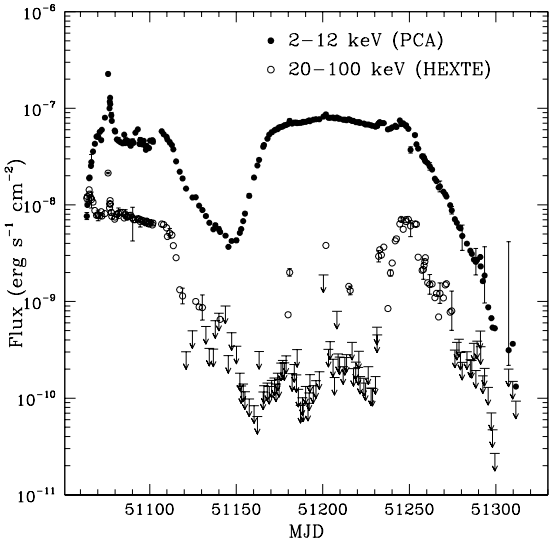

Figure 1. PCA and HEXTE light curves of the 1998/1999 outburst of XTE J1550-564 from [8].

spectral evolution of the system. In Fig. 2 the CCD of XTE J1550-564 from [9] is shown. The colors are defined in such a way that the diagram preserves linearity, meaning that the sum of two models will result in a position lying between the points characterizing those models. The position of disk-blackbody models with different temperatures and power-law models with different photon indices are shown. Notice that the disk-blackbody points lie on a roughly vertical line, while the power-law line is much more inclined. This means that changes in the parameters of the two models are almost decoupled in this diagram. In Fig. 2, panel B refers to the times after MJD 51259, when the PCA gain was changed. Looking at panel A, we can follow the evolution the spectral distribution and, assuming the spectrum can be approximated with the sum of these models, we can have an idea of the state transitions.

At the beginning of the outburst the points are away from the DBB line, indicating the presence of a substantial amount of power law. Being the total flux relatively low, we can tentatively call this an IS. Then the source moves very close to the DBB line and slowly moves up, increasing the temperature of the DBB component: a HS. What

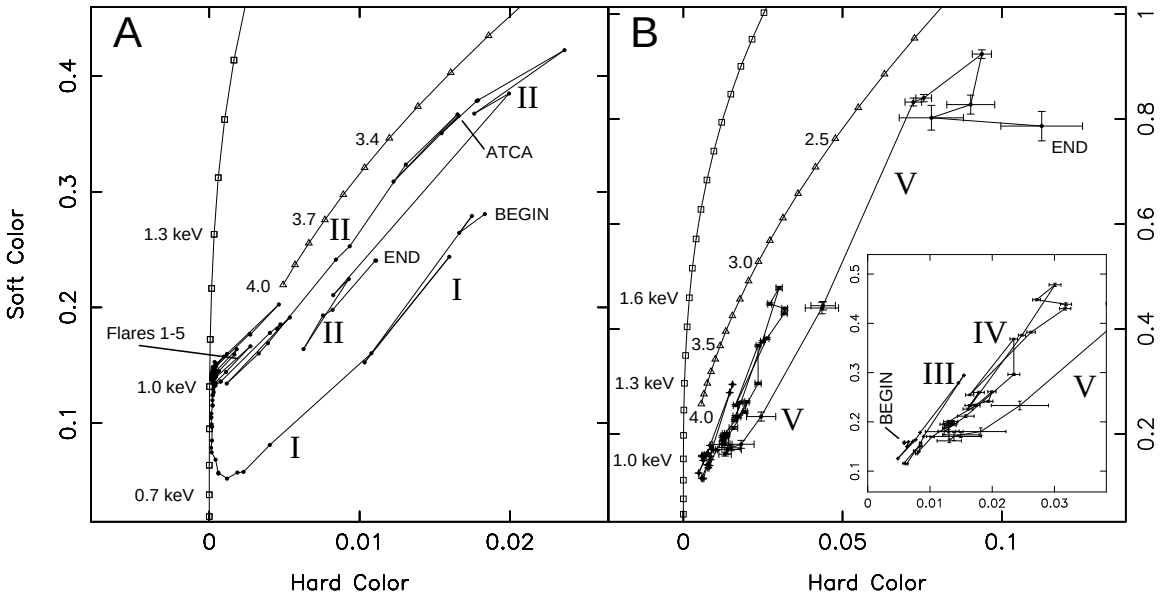

Figure 2. Color-color diagrams for the second part of the 1998/1999 outburst of XTE J1550-564 (from [9]). Panel A and B are for different gain epochs of the PCA detector. Open symbols, squares and triangles, mark the position of disk-blackbody and power law models respectively.

follows is the flaring which can be seen in the HEXTE light curve in Fig. 1, corresponding to large deviations from the DBB line: VHS excursions. Overall, the evolution can be deconvolved in this way: the temperature of the soft component first increases then decreases smoothly, moving the source firs up then down in the diagram. The power law component changes in intensity in a rather uncorrelated way, bringing first the source close to the DBB line (small power-law contribution), then moving it away repeatedly during the flares. Looking at the timing properties, we see a PDS typical of a HS when the source is close to the DBB line, and extremely complex power density spectra, dominated by multi-peaked QPOs, when the contribution of the power law increases, strengthening the state identification. At the very beginning and at the very end of the outburst, when the power-law component dominates the flux, the PDS is characteristic of the LS [9, 15].

What we have seen above is not what the simple picture of state transitions driven by accretion rate would predict. There are state transitions, but they seem to be decoupled from accretion rate. Figure 3 shows a schematic description of this (from [9]). While changes in the accretion rate are naturally responsible for variations in the temperature of the soft component (corresponding to large changes in detected flux), the power law component moves along different branches and transitions to the VHS can happen at different values of the accretion rate. On the contrary, the LS appears only at the beginning and at the end of the outburst, suggesting a connection to low accretion rates.

4. Spectral/timing states II

What shown above has important consequences for the picture of spectral/timing states. The first, already mentioned, is that state transitions in BHC are not driven *only* by mass accretion rate: a second independent parameter is needed. It is not in the scope of this paper to discuss physical possibilities for what this second parameter is. In GS 1124-68, the transitions were relatively simple and a sequence of states was identified [6], while here things behaved in a more complex fashion. Other sources, like GS 2023+338 [2], remained in the LS despite large changes in ac-

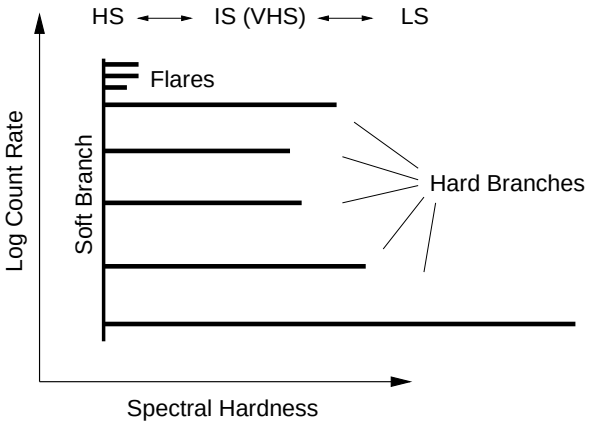

Figure 3. Diagram of the state behavior of XTE J1550-564 from [8].

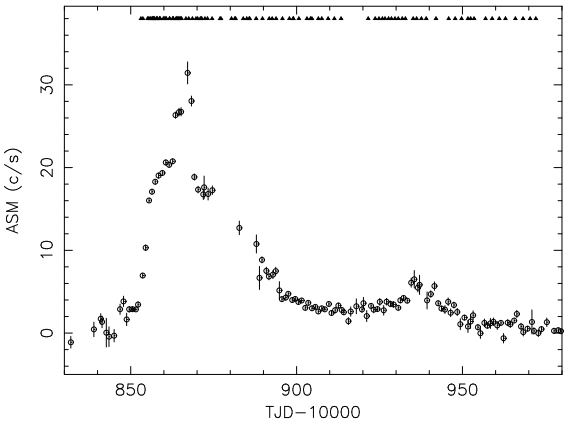

Figure 4. RXTE/ASM light curve of the 1998 outburst of 4U 1630-47. The triangles mark the dates of the PCA pointed observations. From [18]

cretion rate, indicating that this second parameter did not vary. On the contrary, in the 1996 transition of Cyg X-1, a relatively small change in accretion rate was sufficient to trigger a state transition [1]. The second consequence is that the IS becomes indistinguishable from the VHS, since its spectral/timing properties were identical to those of the VHS, the difference being only in the range of accretion rate at which it appeared [7, 16]. If the VHS can be triggered at any accetion rate, no IS is needed. This brings the number of states of black hole candidates back to **three**.

5. 4U 1630-47

4U 1630-47 is a bright recurrent transient system that shows an outburst roughly every 600 days (see [17]). Since the launch of RXTE, it has showed four outbursts; here I concentrate on the second one, during 1998. The outburst light curve is shown in Fig. 4, and the corresponding CCD (defined in a similar way to that of XTE J1550-564 above) can be seen in Fig. 5 (both figures are from [18]).

In the case of 4U 1630-47, all points in the CCD lie close to the power-law line. The fact that the source moves from below to above that line indicate changes in the temperature of the soft component, but we never see a state dominated by it like in the case of XTE J1550-564. This can also be seen from the complete spectral analysis in [19]. The data from [18] indicate that the source was always in the VHS. During the final stages of this outburst, the source entered the LS, as expected (see [20]). A parallel timing analysis shows indeed that the HS seems not to be entered at any time during this outburst. As in the case of XTE J1550-564, the VHS power spectra appear to be extremely complex and difficult to interpret [18].

In the case of 4U 1630-47, it is difficult to extract from the CCD information about the evolution of the mass accretion rate. However, five observations during this outburst were made with BeppoSAX during the decay part of the outburst (between TJD 10864-10899): detailed spectral analysis with a DBB plus power law model indicate that the data are consistent with no variation in the mass accretion rate [21]. Of course this result is strongly model-dependent, but it suggests that rather large changes in the timing properties (see [18]) can appear without being driven by strong variations in the mass accretion rate.

6. GRO J1665-40

GRO J1655-40 is one of the first two microquasars (see [22]). RXTE observed a major outburst of this source in 1996 (see [23, 24]). The RXTE/ASM light curve for this outburst is

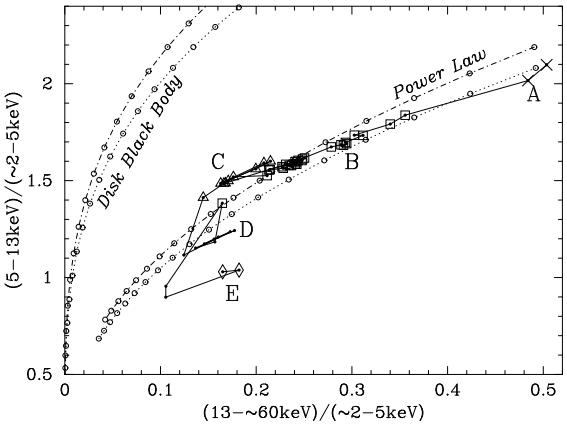

Figure 5. CCD of the 1998 outburst of 4U 1630-47. The outburst proceeds from A to D. From [18].

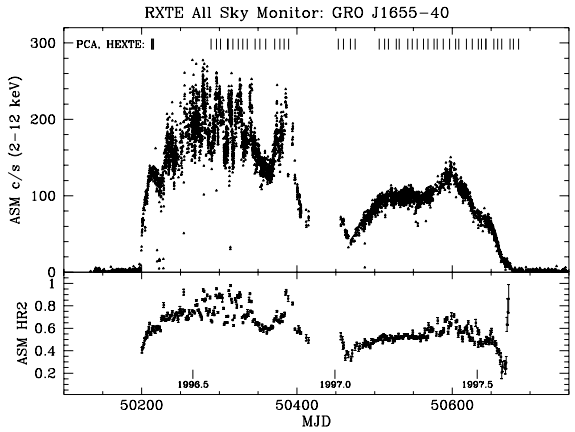

Figure 6. RXTE/ASM light curve of the outburst of GRO J655-40 (from [23]). The bottom panel shows the corresponding ASM hardness ratio. The different states are indicated.

shown in Fig. 6. The outburst evolution looks similar to that of XTE J1550-564, with two separate parts, the second of which looks smoother than the first. Spectrally, three states could be identified: VHS in the first part of the outburst, HS in the second, with the exception of the last

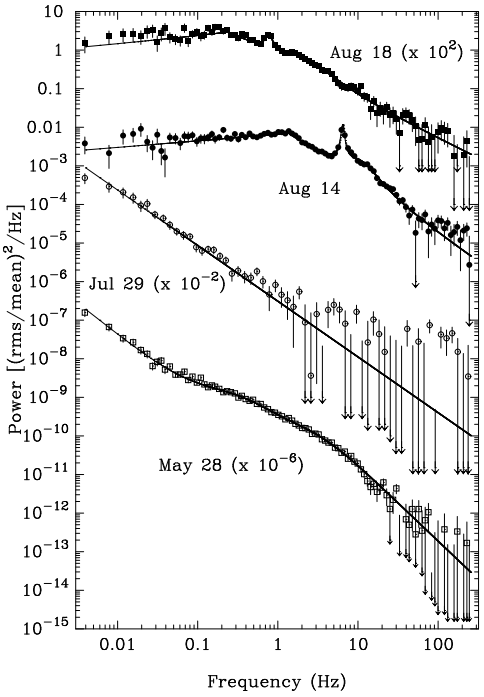

Figure 7. Four Power spectra at the end of the outburst of GRO J1655-40. From [25]).

PCA observations, when the source switched to the LS ([24]). In the timing domain, things did not look that simple. The only major difference between the first and the second part of the outburst was the presence of QPO features in the former [23]. You can see the overall shape of these PDS in Fig. 7, where four PDS at the end of the outburst are shown (from [25]). The typical PDS for the source, QPOs excluded, is the bottom one, with a few % fractional variability. In a month time the source moved to a HS-like PDS and then to a typical PDS for a LS (see Fig. 7).

From this, the question arises: how is the VHS defined in the PDS domain? We have given a definition in Section 1, but after that we have different and complex PDS which we classified as VHS. This will be discussed later in this paper.

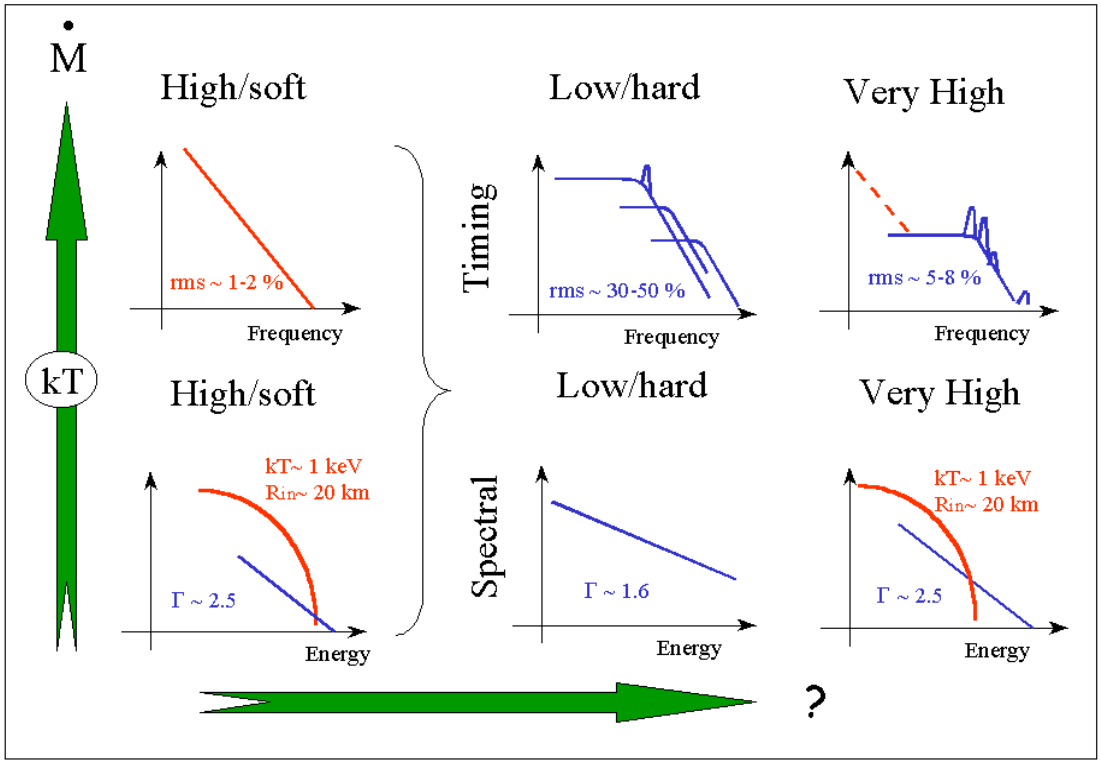

Figure 8. Spectral/timing states and their dependence on mass accretion rate and the second (unknown) parameter.

7. Spectral/timing states III

From what we have seen, we can summarize a few points about states and state-transitions:

- The soft disk component reacts to changes in the accretion rate, the hard component (a power law in the 2-20 keV band) reacts to something else (indicated as a question mark in Fig. 8).
- The LS is observed only at the beginning and at the end of the outbursts, indicating its association with a low accretion rate
- The main difference between VHS and HS is the presence of the hard component: if it is present, significant short-term variability is observed and the source is in the VHS. If it suppressed or absent, there is little variability and the source is in the HS. As indicated above, the appearance of the hard component is driven by a second parameter whose nature is not clear.
- It must be noted that it is not at all clear that the power-law components observed in the VHS and in the HS are the same component. In order to verify this, high-energy coverage is necessary, to check for the presence/absence of a high-energy cutoff (see [26]). In the case of GRO J1655-40, orbit-related absorption dips were observed: during these dips, both the disk and the power-law component were heavily absorbed, and an additional weak steep power law was visible [27]. It is possible that this component is the HS power law, which would only

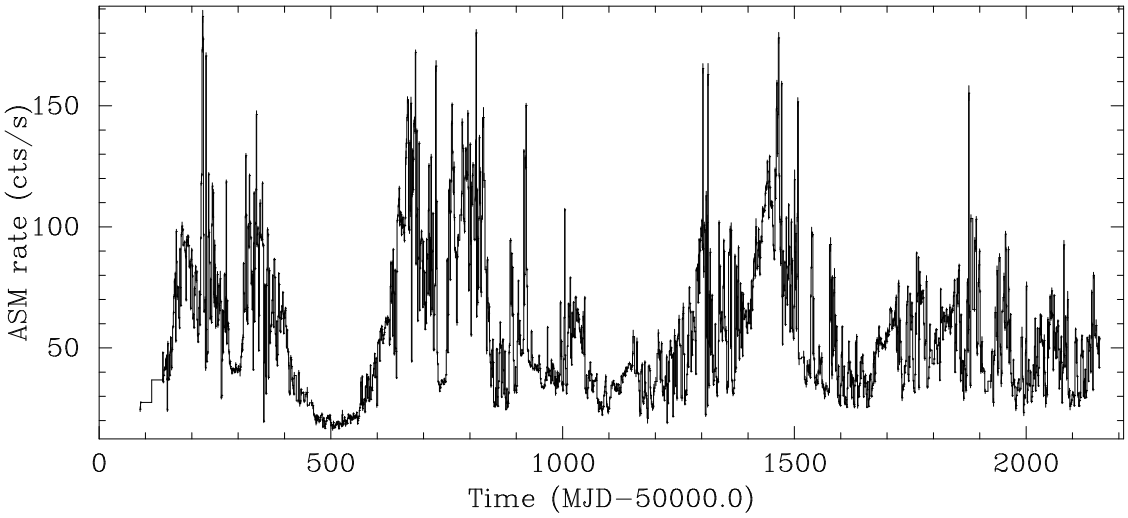

Figure 9. RXTE/ASM light curve of GRS 1915+105 (updated to 2001 September 6). Bin size is 1 day. 1 Crab $\sim$ 75 cts/s.

become detectable when the other much brighter hard component disappears.

As mentioned above, the phenomenological description of the VHS needs to be discussed. We have seen very different PDS associated to this state, which are much more complex than what shown in Fig. 8. Indeed, it would be hard to describe a typical PDS for the VHS. In the timing domain, the difference with the HS is the presence of significant variability, whether in the form of continuum components or QPOs, above the 1-2% observed in the HS. This variability is associated to the hard component and not to the softer disk component, and indeed it is not observed when the hard component is missing.

8. GRS 1915+105

The systems examined so far had properties that were not too different from those mentioned in Sect. 1 for a well-behaved transient: their outburst was a few months long, although more complex than a fast-rise/exponential decay, and they underwent state transitions in the course of the outburst. The original microquasar, GRS 1915+105 did not behave equally well. As an X-ray source, it appeared in the sky in 1992 [28] and remained bright since then.

Figure 9 shows the RXTE/ASM light curve of GRS 1915+105: it shows very marked variability, like the first part of the outburst of GRO J1655-40. However, unlike in the case of GRO J1655-40 (see [23]), this variability extends to very low time scales [30, 31, 34]. This can be seen in Fig. 10, where a few examples of RXTE/PCA light curves, binned at 1 second, are shown.

This extraordinary variability has been interpreted as due to the repeated transitions between three basic states, called states A, B and C [34]. A scheme of transitions between these states is shown in Fig. 11 (from [34]). Is there a relation between these three states and the three canonical states described above? Of course, transitions as fast and repeated as those shown in Fig. 10 are not observed in any other source, but the similarities might be stronger than the differences. In order to answer, we need to examine the states of GRS 1915+105 in more detail:

- *State B*: The energy spectrum consists of the superposition of a strong soft thermal component (with kT$\sim$2 keV) and a steep hard component $\Gamma \geq 3$. The PDS is steep, bumpy, with a total fractional variability in the 5-10% range.

- *State A*: The energy spectrum is similar to

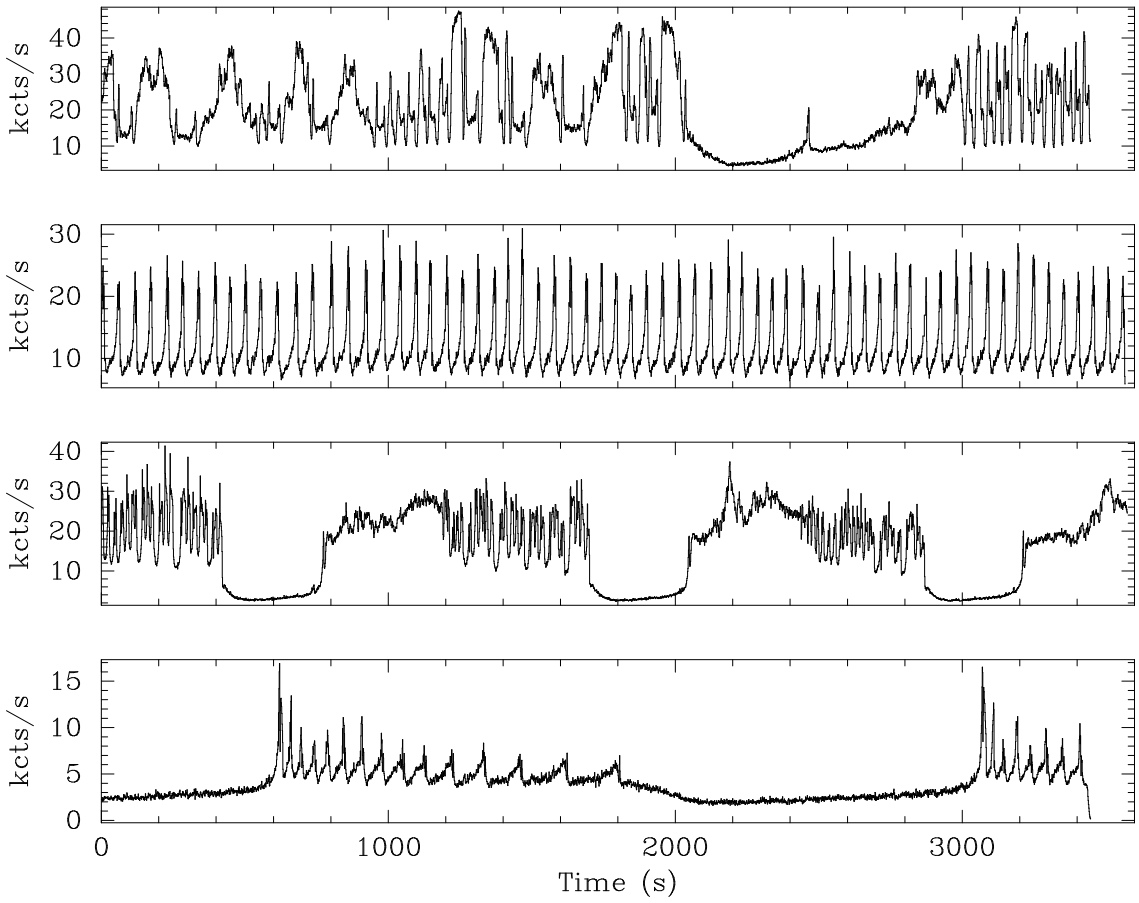

Figure 10. Four examples of one-hour RXTE/PCA light curves of GRS 1915+105. Bin size is 1 second.

that of state B, but softer. This difference is attributed by [34] to a softer temperature of the thermal component. The PDS is a bumpy power law, with fractional rms lower than state B.

- *State C*: The energy spectrum is dominated by the hard component, which is considerably flatter than in the other states, with Γ that can be as low as 1.8. The PDS shows a band-limited noise component with a variable break frequency (between 0.07 Hz and a few Hz). A low-frequency QPO is always present, with a centroid frequency strongly correlated with count rate and spectral hardness [29].

As one can see, states A and B seem to have something in common with the canonical VHS, while state C shows similarities with the LS, although the dependence of the timing parameters with rate and hardness is something that was seen before in the VHS of GS 1124-68 [32]. In addition, by combining RXTE and CGRO/OSSE data, [33] showed that the broad-band spectrum of GRS 1915+105 in states C and B does not show any evidence of a high-energy cutoff (see Fig. 12, unlike typical BHC in the LS (see [26]).

At this stage, it is difficult (and dangerous) to claim any strong association between the three states of GRS 1915+105 and the canonical states of more conventional systems. The source is extremely bright and possibly what we see is only intances of VHS at very high accretion rates.

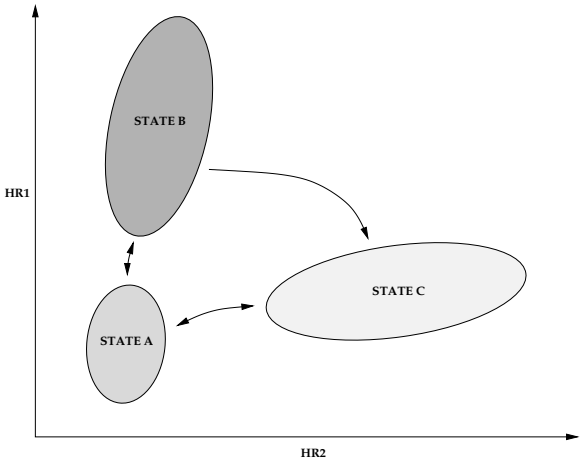

Figure 11. Schematic color-color diagram showing the allowed transitions between the three states of GRS 1915+105. From [34].

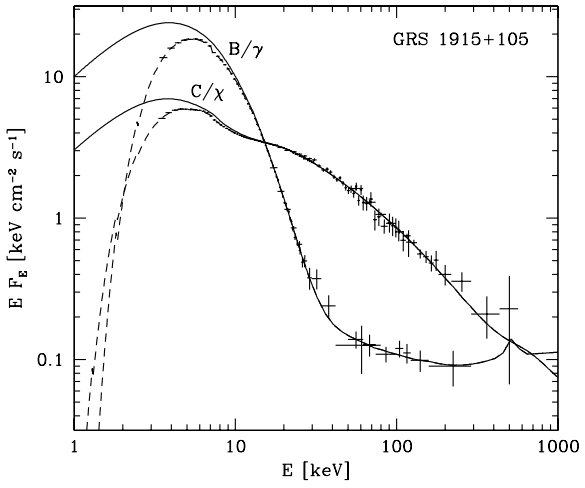

Figure 12. Model spectra for the combined PCA/HEXTE/OSSE spectral fits of GRS 1915+105 in B and C state. No high-energy cutoff is needed for either spectra. From [33].

9. On the timing noise in the LS and in the VHS

As discussed above, there are indications that the hard components in the LS and in the VHS are different, as a high-energy cutoff is detected in the LS, but no high-energy cutoff is detected in the VHS [26]. However, if one looks at the properties of the band-limited noise detected in these two states, such as the correlation between flat-top and break frequency in the PDS, the VHS points lie on the high-frequency extrapolation of the LS ones ([16], see Fig. 13). This is difficult to understand if the two components have a different physical origins: in this case both the characteristic noise frequency and the total fractional rms (see [35]) must be associated either to geometrical parameters or to the thermal disk component.

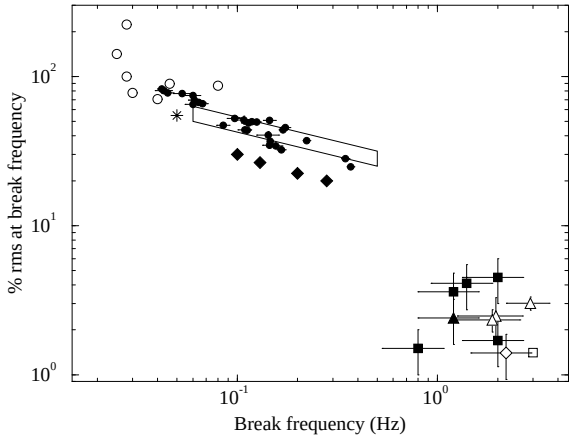

Figure 13. Flat-top level (in fractional rms) vs. break frequency for a sample of BHC. LS points are clustered in the upper left, VHS points in the lower right. From [16].

10. Spectral/timing states: conclusions

Since the launch of RXTE, thanks to the presence of the ASM and the operational flexibility of the mission, the available X-ray data on black hole candidates, especially transient systems, as increased substantially. The picture that emerges from the analysis of this large database is at the same time simpler and more complex than the paradigm that existed before. It is more com-

plex because the phenomenology became quite complicated. The variety of QPOs observed in XTE J1550-564 and GRS 1915+105, and the extreme structured variability of the latter are perhaps the best examples. However, it also became somewhat simpler, as the number of basic spectral/timing states is now reduced to three, despite the tremendous diversity of some timing features, and the presence of a second parameter governing state transitions (although its physical nature needs to be addressed) might yield a direct measurement of a fundamental parameter of these systems. Among all sources, GRS 1915+105 shows more variability and state-transitions than all other sources together. it might be the way to solving basic problems of accretion, but it might also turn out to be an endless complication that leads away from the solutions. However, it is important that theoretical models address the general picture described above in addition to trying to describe in extreme detail the spectral distribution of a particular state in a particular source, especially since any spectral fit to low-resolution data involves by definition a strong a priori bias.

REFERENCES

1. Zhang, S.N. *et al.* 1997, ApJ, 477, L95.
2. Tanaka, Y., Lewin, W.H.G. 1995, in "X-ray Binaries", Cambridge Univ. Press, p126
3. van der Klis, M. 1995, in "X-ray Binaries", Cambridge Univ. Press, p252
4. Miyamoto, S. *et al.* 1993, ApJ, 403, L39.
5. Miyamoto, S. *et al.* 1994, ApJ, 435, 398.
6. Ebisawa, K. *et al.* 1994, PASJ, 46, 375.
7. Belloni, T. *et al.* 1997, A&A, 322, 857.
8. Sobczak, G. *et al.* 2000, ApJ, 544, 993.
9. Homan, J. *et al.* 2001, ApJS, 132, 377.
10. Bradt, H.V., Rothschild, R.E., Swank, J.H. 1993, A&AS, 97, 355.
11. Swank, J. 1998, Nucl. Phys. B. (Proc. Suppl.), 69, 12.
12. Levine, A.M. *et al.* 1996, ApJ, 469, L33.
13. Zhang, W. *et al.* 1993, Proc. SPIE, 2006, 324.
14. Jahoda, K. *et al.* 1996, Proc. SPIE, 2808, 59.
15. Cui, W. *et al.* 1999, ApJS, 512, L43.
16. Méndez, M. & van der Klis, M. 1997, ApJ, 479, 926.
17. Kuulkers, E. *et al.* 1997, MNRAS, 291, 81.
18. Dieters, S. *et al.* 2000, ApJ, 538, 307.
19. Trudolyubov, S.P. *et al.* 2001, MNRAS, 322, 309.
20. Tomsick, S.P. & Kaaret, P. 2000, ApJ, 537, 448.
21. Oosterbroek, T *et al.* 2000, A&A, 340, 431.
22. Hjellming, R.M. & Rupen, M.P. 1995, Nature, 375, 464.
23. Remillard, R.A. *et al.* 1999, ApJ, 522, 397.
24. Sobczak, G. *et al.* 1999, ApJ, 520, 776.
25. Méndez, M., Belloni, T., & van der Klis, M. 1998, ApJ, 499, L187.
26. Grove, J.E. *et al.* 1998, ApJ, 500, 899.
27. Kuulkers, E. *et al.* 1998, ApJ, 494, 753.
28. Castro-Tirado, A.J., Brandt, S., Lund, N. 1992, IAUC, 5590.
29. Reig, P. *et al.* 2000, ApJ, 541, 883.
30. Greiner, J., Morgan, E.H., Remillard, R.A. 1996, ApJ, 473, L107.
31. Morgan, E.H., Remillard, R.A., Greiner, J. 1997, ApJ, 482, 993.
32. Takizawa, M. *et al.* 1997, ApJ, 489, 272.
33. Zdziarski, A. *et al.* 2001, ApJ, 554, L45.
34. Belloni, T. *et al.* 2000, A&A, 355, 271.
35. Belloni, T., Psaltis, D., van der Klis, M. 2001, ApJ, submitted.

ACKNOWLEDGEMENTS

I thank the Cariplo Foundation for financial support.